Journal of Applied Physics
AIP Publishing

Study of Flash Lamp Annealing to Promote Crystallization of Indium Tin Oxide Thin Films

Ethan Neitzke[1*], Qi Hua Fan[1,2]

[1]Department of Electrical and Computer Engineering, Michigan State University, East Lansing, MI, USA
[2] Department of Chemical Engineering and Materials Science, Michigan State University, East Lansing, MI, USA

***Abstract*—** The use of flash lamp annealing as a low temperature alternative or supplement to thermal annealing is investigated. Flash lamp annealing and thermal annealing were conducted on 100 nm thick indium tin oxide (ITO) films deposited on glass to compare the films properties under different annealing methods. The ITO samples had an initial sheet resistance on average of 50 Ω/sq. After flash lamp annealing only the sheet resistance was reduced to 33 Ω/sq, while by thermal annealing at 210°C for 30 minutes a sheet resistance of 29 Ω/sq was achieved. Using a combination of flash lamp annealing and thermal annealing at 155°C for 5 minutes a sheet resistance of 29 Ω/sq was achieved. XRD analysis confirmed that flash lamp annealing can be used to crystallize ITO. Flash lamp annealing allows for the low temperature crystallization of ITO on a time scale of 1-3 minutes. Through electrical and optical characterization, it was determined that flash lamp annealing can achieve similar electrical and optical properties as thermal annealing. Flash lamp offers method of low-temperature annealing which is particularly suitable for temperature sensitive substrates.

I. INTRODUCTION

Indium tin oxide (ITO) is a type of transparent conductive oxide (TCO) that has many uses in solar cells, optoelectronic devices, flexible electronics, LEDs, etc. [1-4]. ITO films can be produced by a variety of methods including chemical vapor deposition, dc and rf magnetron sputtering, evaporation, and spray pyrolysis [5, 6]. All the deposition methods for ITO require an elevated temperature ranging from 300 – 500°C in order to crystallize the material and produce a high-quality film. References [5, 6] have provided detailed information on the various deposition methods. An alternative to depositing the material at an elevated temperature is to deposit at room temperature then thermally anneal the substrate post process in order to crystallize the film [2, 5-7]. The high temperature needed to produce quality ITO films leads to higher costs and limits the potential substrates that can be used. For some applications like flexible electronics and displays [5, 8] it is desirable to deposit ITO on flexible polymers such as polyethylene terephthalate (PET) or polyethylene naphtholate (PEN). However, elevated temperatures are needed to produce a quality film, which is not possible for many polymers [2, 7, 8]. To produce high quality ITO thin films on flexible polymers a low temperature method is needed.

Thermal annealing (TA) post deposition has often been used to produce the desired optical and electrical properties for ITO films [7]. Some groups have suggested ultra-short laser treatment as an alternative to crystallize ITO films on flexible polymer substrates [5]. Another possibility for low temperature processing is flash lamp annealing (FLA) also known as intense pulsed light annealing (IPL), photonic curing, or photonic sintering [1]. FLA has been around for many years and been used in the semiconductor and solar cell industry as well as for the processing of printed electronics [1, 9-11]. FLA has been of interest in the solar cell and printed circuit industry due to its short processing time and ability to be used for thermally sensitive devices [1, 9]. [12] was able to use IPL to reduce the post-metallization annealing time of silicon heterojunction solar cells from minutes to seconds. There are several published works on using flash lamp to anneal/crystallize ITO thin films [13, 14]. [13] focuses on how the FLA parameters affect the ITO film properties. [14] focuses on the process of FLA and how to improve absorption in the ITO film.

This work compares the similarities and differences between TA and FLA annealing as well as a sequential TA and FLA treatment. The benefits of combined TA and FLA treatment of ITO are discussed, which serves as a paradigm for low temperature processing in the semiconductor and solar industry.

In FLA an intense microsecond to millisecond pulse of electromagnetic radiation is exposed to the substrate. Xenon lamps are typically used for FLA, the spectrum of the lamp used in this study can be found in figure 1. The xenon spectrum shows that the radiation produced ranges from ultraviolet to near-infrared, with the visible spectrum being the most

* Corresponding author E-mail: neitzkee@msu.edu

intensive. During FLA operation, a capacitor bank is charged up to the desired voltage then discharged by the xenon lamp which delivers the energy to the substrate in the form of photons. The substrate absorbs the electromagnetic radiation which leads to the heating of the substrate [1]. The voltage of the capacitor bank largely determines the energy density of the light that is delivered to the sample [9]. In figure 1 it can be seen how the voltage of the capacitor bank affects the intensity of the pulses. The duration, frequency, voltage, duty cycle and number of pulses can all be controlled to fine tune the energy transferred to the film. The intense light absorbed by the films causes significant short-lived temperature increases [9]. The light energy absorbed excites the electrons which interact with phonons that then disperse the energy throughout the lattice [9]. The pulse duration of the flash is typically under a millisecond so there is no significant time for the heat generated in the film to be transferred to the substrate [8]. To ensure the substrate does not get damaged during the FLA process the discharge parameters can be adjusted to limit the heating of the substrate [8].

In [15] Wünscher et al investigate different post-deposition sintering processes for production of flexible electronics. FLA is appealing for flexible electronics since it allows for targeted heating of the ink while leaving the substrate largely unaffected [15]. To ensure that FLA operates as a localized heating method and prevents damage to the substrate it is crucial to have the pulse length much shorter than the time required for thermal equilibrium to be achieved between the ink layer and the bulk substrate [15]. In [11] Abbel, Robert, et al were able to show that FLA can work in roll-to-roll applications. FLA has shown promise as a fast and low temperature annealing method which makes it appealing for many applications such as ITO film crystallization.

In this study, the properties of ITO films deposited on glass at room temperature post processed by traditional thermal annealing and FLA were characterized. The properties of FLA ITO films were investigated to determine if FLA can produce the same quality of films as TA and whether a sequential treatment could produce higher quality films. How the annealing methods affected the films electrical properties, optical properties and morphology were investigated. In addition to FLA the combination of both TA and FLA is investigated to determine if there are any significant changes to the properties of the films. This study has validated the feasibility of FLA as a low-temperature alternative to promote the crystallization of ITO films.

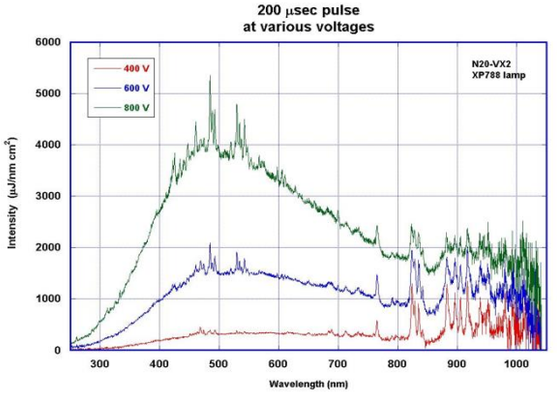

Figure 1. Spectrum of N24-VX2 xenon lamps

II. EXPERIMENTAL DETAILS

100 nm thick ITO films were deposited on 153 × 153 mm^2 glass substrates with a thickness of 300 μm. The films were deposited by DC magnetron sputtering in an argon gas at a pressure of 3 mTorr (0.4 Pa) at room temperature. Prior to the deposition the vacuum system was pumped down to a pressure of 1×10^{-6} Torr (133 μPa) and underwent pre-sputtering for 10 minutes; the power density was approximately 20 W/m^2. The ITO-coated glass substrates were cut into 12 × 12 mm^2 square samples for subsequent treatment and characterization. The original sheet resistance of each sample was measured using a 4-point probe (Guardian Manufacturing SRM-232-1000). Three methods were used to process the ITO films in order to compare FLA to TA and the combination of both.

The first procedure involved only FLA with all variable's constant except the number of pulses. The flash conditions were as follows; the voltage was 820V, 90% duty cycle, 1 micro pulse per pulse with a 265 μs pulse length, 2 Hz frequency and a pulse count which was varied as 20, 50, 100 and 200. Simulation of the flash lamp process was done using the Novacentrix SimPulse software to get an understanding of the process parameters and the temperature profile of the sample. Three samples were used for each TA condition; one of these samples then underwent FLA treatment. Each sample was measured multiple times at different locations to ensure the data was reliable. The FLA experiments were conducted in air at atmospheric pressure using a Novacnetrix PF-3300 flash lamp system which utilized three N24-VX2 xenon lamps. For the first procedure, the samples were placed in the Novacentrix system and preheated at 100 °C for 3 minutes before FLA to prevent the film from being thermally shocked by the FLA. After the FLA treatment, the samples were left in the system to cool to 70 °C before they were removed to prevent a quenching-like effect from the flash lamp.

The second annealing procedure involved only thermal annealing. Three samples were annealed in an oven (Across International ACCUTEMP-09) at atmospheric conditions. The oven was preheated to the desired temperature then the samples were put on preheated trays and placed inside the oven. A k-type thermocouple was used to monitor the actual temperature locally on the sample tray. Samples were annealed at three temperatures: 155°C, 190°C, and 215 $°C$. At each temperature the samples were annealed for 5, 15 and 30 minutes. When the samples were taken out of the oven, they were left to cool on the trays for 5 minutes before being removed.

For the third annealing procedure, the samples first underwent thermal annealing following procedure two, then the samples underwent FLA using the conditions described in procedure 1 but with a constant pulse count of 100.

After annealing, the samples electrical, optical, and structural properties were characterized. Guardian 4-point probe was used to measure sheet resistance. Mobility and carrier concentration were measured using a Lake Shore Cryotronics HMS-TT FastHall station. Transmittance and reflectance were measured using a UV-Vis-NIR spectrophotometer (KLA Instruments, F20) with a resolution of approximately 1 nm. Glancing angle x-ray diffraction (XRD) was performed on a Rigaku SmartLab system at an incident angle of 1° using Cu Kα radiation having a wavelength of 1.54 Å, power of 1200 W and a scan rate of 2.4°/min. The morphologies of the samples were investigated by SEM with an accelerating voltage of 3 kV (Carl Zeiss, Auriga Dual Column Focus Ion Beam SEM). The film thickness was measured using a (Brunker DektakXT) profilometer with a 6.5 μm tip, and a stylus force of 10 mg.

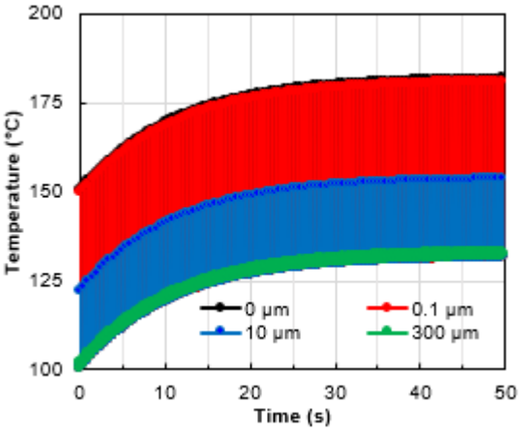

Figure 2. Novacentrix Convective Temperature profile simulation, showing temperature at different depths in the substrate for a pulse

III. RESULTS AND DISCUSSION

The flash lamp annealing process was simulated using Novacentrix SimPulse Software to estimate the substrate temperature profile. The SimPulse Software uses a 1-D heat conduction model to predict the temperature profile throughout the film stack; for a more in depth understanding of the model see [16]. The flash conditions used were 820V, 90% duty cycle, pulse length of 265 µs at a frequency of 2 Hz. The total pulse count was varied as 20, 50, 100 and 200 while all other process parameters were held constant. Using the SimPulse software the temperature at various depths in the film and substrates were simulated for 100 pulse counts as shown in figure 2, where there is a pulse every half second so 50 seconds corresponds to 100 pulses. The temperature profile was monitored at the surface of the ITO layer (0 µm), the end of the ITO layer (0.1 µm), 10 µm into the glass substrate and on the back side of the substrate as shown in figure 3. In figure 1, the surface of the film reaches a max temperature of 181.7 °C at the instance of the pulses,

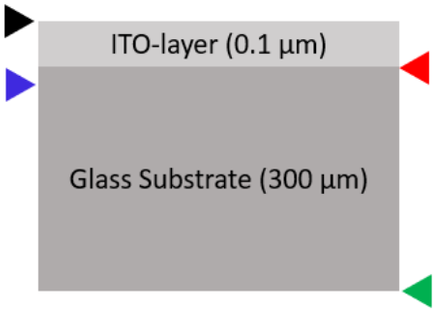

Figure 3. Schematic of film and substrate orientation with depth markers

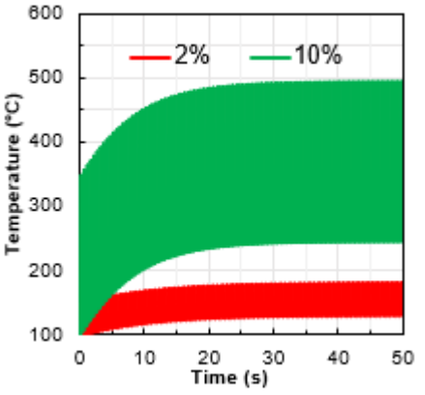

Figure 4. Novacentrix simulation of temperature profile at surface of film for a film with absorption coefficient of 0.02 and

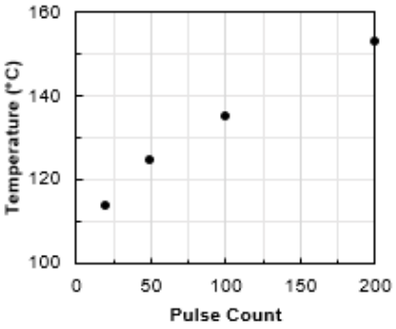

Figure 5. Average temperature at surface of film for increasing pulse counts

while the average temperature is 135.2 °C. At a depth of 10 μm the max temperature is 153.5 °C, while the average temperature is 129.6 °C. The back side of the substrate reaches a max temperature of 133.1 °C with an average temperature of 125.9 °C. Figure 4 shows how the temperature profile of the films changes substantially with the absorption coefficient. Figure 4 shows that the absorption coefficient is very important for determining the flash conditions as significant film temperatures can be reached. For simulation purposes, we used an absorbance of 2.5% since the average absorbance over the visible spectrum (400-800nm) was 2.5% based on transmission and reflectance measurements taken of the as-deposited sample. We only considered the visible spectrum since this is the range over which the xenon lamps are the most intensive. The average temperature at the film's surface for increasing the pulse counts can be seen in figure 5. The max temperature is achieved at the instance of the pulse after which the temperature drops rapidly before the next pulse. Due to the short duration of the pulse measuring the actual instantaneous temperature profile is difficult and thus the temperature profile is based only on the simulation. The energy delivered to the film during the pulse quickly disperses throughout the film which accounts for the average temperature of the substrate.

XRD measurements for the various annealing conditions can be found in figure 6. The XRD diffraction peaks in figure 6(a) proves that FLA can be used to crystallize the ITO. For all annealing methods the (222) plane scatters the most intensively. For a pulse count of 20 or 50 only the (222) plane can be seen in the XRD patterns. For higher pulse counts of 100 and 200 there are additional peaks corresponding to the (211), (400), (440), and (622) planes which, along with the (222) plane, are all characteristic of ITO films as seen by other work [6, 7, 17, 18]. The intensities of the peaks increase with the pulse counts, indicating a more crystalline film. Figure 6(d) shows that thermal annealing at 155°C, 190°C or 215°C for

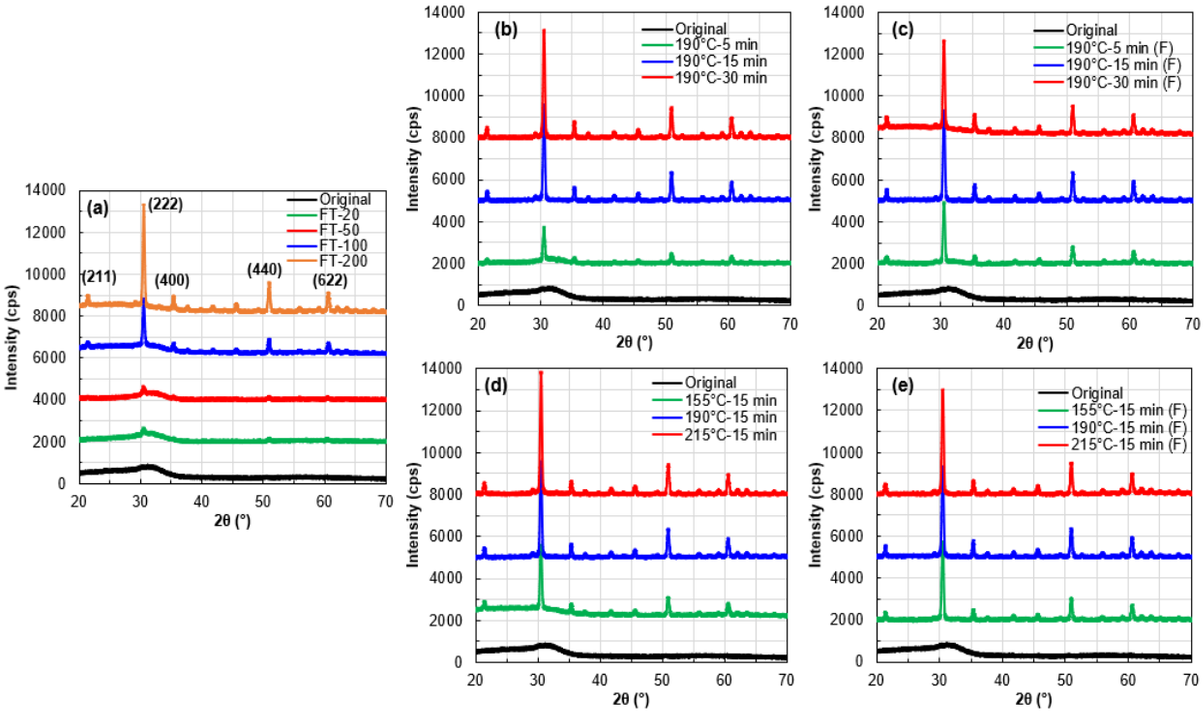

Figure 6. XRD diffraction patterns for a) FLA treatment at different pulse counts b) TA at 190°C for different times c) TA and FLA at 190°C for different time d) TA at different temperature e) TA and FLA at different temperatures

15 minutes can crystallize the film and that higher temperature leads to higher intensities in the XRD pattern. Figure 6(b) illustrates that longer annealing times leads to higher diffraction intensities, which means an enhanced crystallization. Comparing figures 6(b, d), to 6(c, e) it is apparent that the addition of flash lamp annealing after thermal annealing only aids in the crystallization of ITO if the thermal annealing step was short. The sample annealed at 190 °C for 5 minutes saw more intensive XRD peaks particularly at the (222) plane after FLA. The most intensive scattering was achieved for sample TA at 215°C for 15 minutes. FLA at a pulse count of 100-200 can produce the same XRD diffraction intensity as TA at 190°C for 30 minutes which proves FLA is a much faster crystallization method.

The Sherrer formula (equation 1) was used to calculate the crystal size of the samples [17, 18]. λ is the wavelength of the x-ray radiation used in nm. β is the full width at half max (FWHM) in radians. θ is the Bragg angle in radians which corresponds to the peaks in the XRD data. K is a dimensionless factor which for ITO is commonly accepted between 0.89-0.9 [17, 18].

$$\tau = \frac{K\lambda}{\beta \cos\theta} \qquad (1)$$

Using Sherrer's equation the mean crystal size was calculated for each peak for each annealing condition. The crystal sizes for the three of the most intensive XRD peaks at different annealing conditions be seen in figure 7. The mean size of the crystals in the (222) plane was smallest for the pulse count of 20 while for pulse counts of 50, 100 and 200 the crystal size was almost identical at roughly 26 nm. The smaller crystal size for the pulse count of 20 can be attributed to the lower energy being transferred to the film. As more energy is transferred to the film more atoms can diffuse and larger crystals can form. There is no change in crystal size from 50-200 pulses. In the (400) and (440) planes the pulse count of 200 had a larger mean crystal size than the pulse count of 100. The higher the pulse count the more energy is transferred to the film which explains the slightly larger crystal size. Figure 7-c shows that the annealing time does not have any significant effect on the crystal size since all times had roughly the same crystal size. Varying the annealing temperature similarly did not greatly affect the crystal size. The effect of flash lamp on the crystal size after thermal annealing appears to be negligible as for some conditions the crystal size increases slightly and for others it decreases slightly. Overall, the different annealing conditions did not have substantial effect on the crystal size. In [2] Joshi, Salil M., et al found that after annealing at high temperatures up to $750°C$ there was no significant grain growth which concurs with these finding that annealing temperature did not have significant effect on crystal size. Ghorannevis, Z., et al in [17] had crystal size being 25.440 nm for 100 nm thick ITO film, grown by RF sputtering which is similar to what was found in this study for the (211) and (222) planes. Ahmed, Naser M., et al in [19] found that the crystal size in the (222) plane increased with annealing temperature, which was not seen in this study. In their study they annealed the ITO samples at much higher temperatures from $250 - 550$ °C, therefore higher annealing temperatures are needed to promote growth of larger crystals. Given the results of [19] significant energy is needed to promote large grain growth in ITO so FLA would not be suitable.

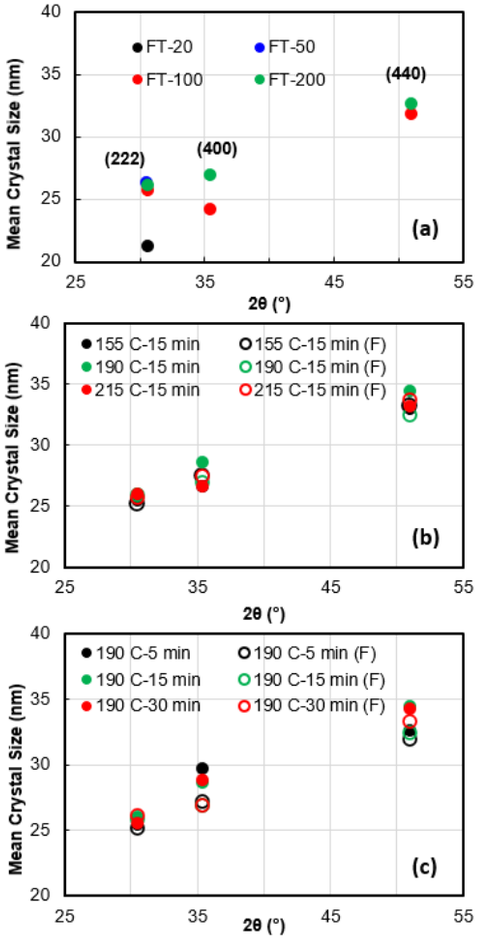

Figure 7. crystal size for a) FLA treatment at different pulse counts b) TA and TA/FLA at different temperatures c) TA and TA/FLA at different times

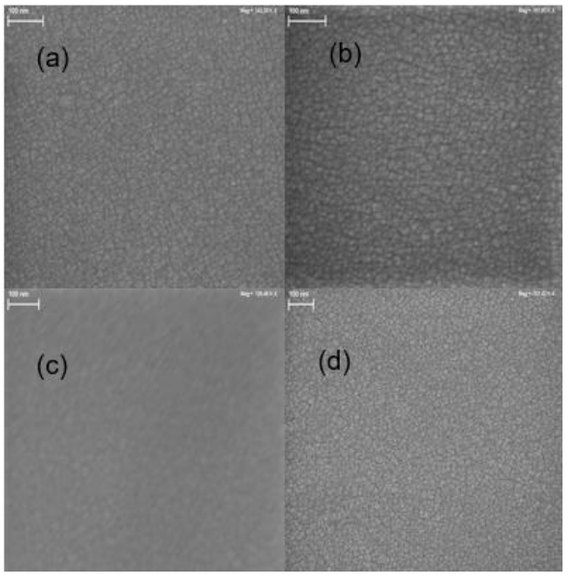

Figure 8: SEM images of flash lamp annealed samples (scale reads 100 nm) a) pulse count 20 b) pulse count 50 c) pulse count 100 d) pulse count 200

The SEM images in figure 8 do not show much difference in the film morphology for the different pulse counts. Images for TA samples similarly revealed no significant structural differences.

Figure 9 shows the carrier concentrations (n) for different annealing treatments. The carrier concentration varied from $3 \times 10^{20}\ cm^{-3}$ to $4.81 \times 10^{20}\ cm^{-3}$. Carrier concentration generally decreased with increased annealing time and increasing temperature. During thermal annealing, defects in the material are removed which affect the charge carriers. Buckeridge et al in [21] suggest that oxygen vacancies act as shallow donors in ITO which contribute significantly to the carrier concentration. [6] states that annealing in air removes oxygen vacancies which act as donors and thus decrease the carrier concentration. The authors in [21-23] label oxygen vacancies as electron donors. Our hypothesis is that the thermal annealing in air removes the oxygen vacancies which act like electron donors and decreases the carrier concentration. The higher the temperature or longer the annealing time the more defects and vacancies are removed and thus the lower the carrier concentration. In figure 9(c) the carrier concentration increases at first for TA at $155°C$. It is believed that this is due to removal of defects that act as traps; not enough energy has been transferred to the film yet to remove oxygen vacancies, but as the time increases the carrier concentration drops again due to removal of those oxygen vacancies. There does appear to be a saturation of the oxidizing effect for TA at $215°C$ as there is no further decrease in n from 15 to 30 minutes as shown in figure 9(c). This saturation of the oxidizing effect is not seen in FLA as the carrier concentration continues to decrease at 200 pulse counts as seen in figure 9(a); perhaps a higher pulse count is needed to see such a saturation.

The carrier concentration initially increases but then decreases after a pulse count of 50 as shown in figure 9(a). During the interval over which the carrier concentration increases is the same as when the mobility remains constant. The hypothesis is that the FLA treatment at low pulse count does not input enough energy into the film to repair defects that require high activation energy, such as impurities or oxygen vacancies; but the low pulse energy is enough to repair dangling bonds at grain boundaries which reduce the recombination rate and thus increases the carrier concentration while leaving the mobility unchanged as seen in figure 10. For higher flash counts and during TA, there is sufficient energy to remove oxygen vacancies which is responsible for the decrease in carrier concentration. Our results agree with the literature which suggests that oxygen vacancies are a major carrier donor in ITO [20, 21]. FLA after TA had no real effect on carrier concentration at $215\ °C$ but further decreased for $190°C$.

Mobility increases after TA or FLA until it reaches a maximum value. For FLA the mobility

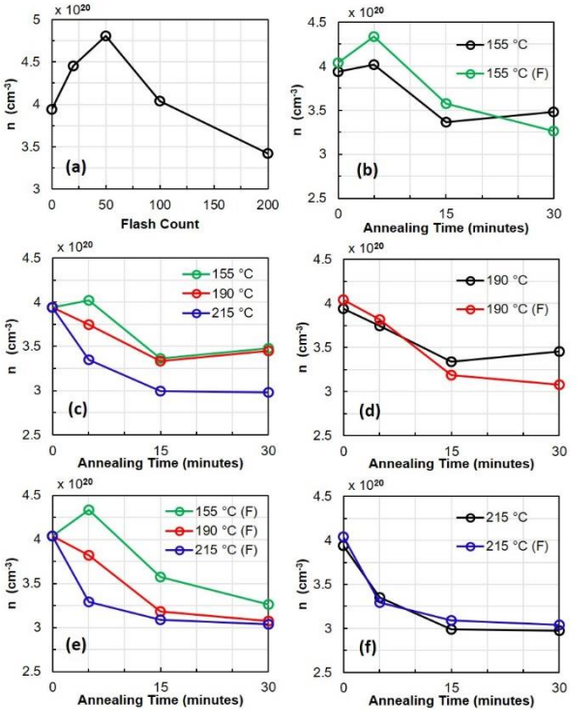

Figure 9. Carrier concentration (scale 10^{20}) as a function of a) flash annealing pulse count c) thermal annealing time and temperature b, d-f) thermal annealing and FLA.

ranged from 35 to 65 $cm^2\,V^{-1}s^{-1}$, while for TA it ranged from 35 to 76 $cm^2\,V^{-1}s^{-1}$ which is similar to values in other literature [20]. The increase in mobility can be attributed to the transition from the amorphous structure of the as-deposited film to the crystallized films produced by TA and FLA as proven by XRD analysis. During the annealing process defects in the lattice are removed; the removal of defects along with the increase in crystallinity allows for higher carrier mobility. Electron mobility can be affected by lattice scattering, neutral impurity scattering, ionized impurity, and grain boundary scattering [7, 20].

The initial change from amorphous to crystalline reduces scattering and recombination due to removal of defects but does not account for the variation in the mobilities. Except for two TA treatments and a FLA treatment with a pulse count of 20 where the average crystal size was slightly smaller for some crystal orientations the average grain size remained almost identical for each treatment condition. Crystal size does not change substantially with the heat treatment so the heat treatment methods presented here mostly aid in the reduction of defects not in crystal growth. The consistency of the grain size suggests that grain boundary scattering is unlikely the main mechanism by which mobility increases. Since the average grain size was roughly the same for all treatment methods; the grain boundary would be roughly the same size so no change in scattering from grain boundaries is to be expected.

Figure 10 shows how the heat treatments affect the mobility. The general trend is that increasing the annealing time or temperature causes the mobility to increase. This increase can be attributed to the reduced defects and thus decreasing scattering. The sample annealed at $215\,°C$ for 30 minutes shows a slight decrease in the mobility. Several mechanisms could contribute to this effect, such as concentrated impurities at grain boundaries due to high temperatures. The actual mechanism needs further characterization.

For FLA, as seen in figure 10(a) the mobility originally remains constant then increases rapidly as high pulse counts. XRD analysis shows the film is barely crystallized for a pulse count of 20 or 50 so the dramatic change in mobility can be attributed to the crystallization at a pulse count of 100. Further FLA at higher pulse counts would increase the crystallinity and remove defects, accounting for the increase in mobility. From figure 10(b, d, f) FLA after TA generally causes an increase in the mobility, which is more pronounced for shorter annealing times. FLA removes additional defects after TA, which decreases scattering.

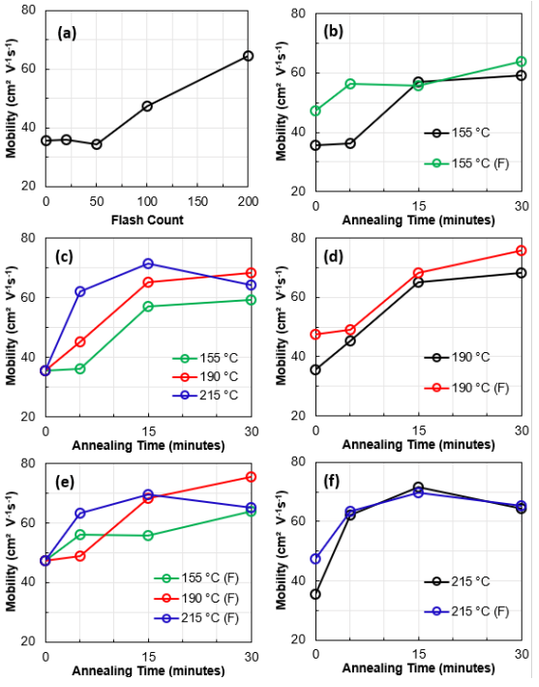

Figure 10. Mobility as a function of a) flash annealing pulse count c) thermal annealing time and temperature b, d-f) thermal annealing and FLA

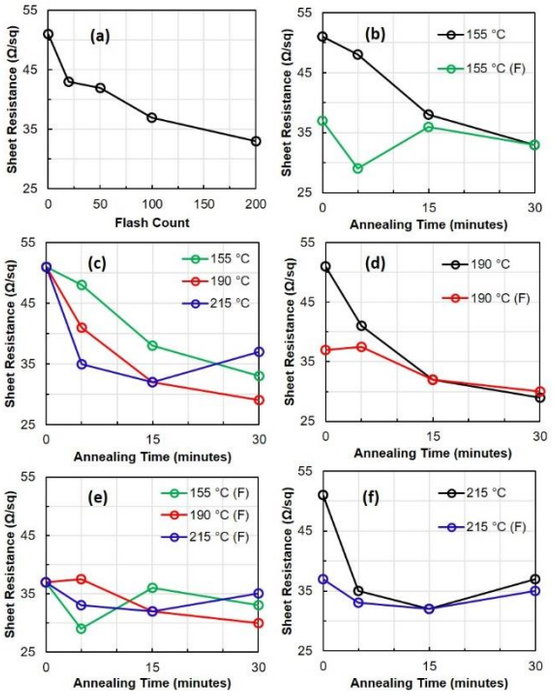

Figure 11. Sheet resistance as a function of a) flash annealing pulse count c) thermal annealing time and temperature b, d-f) thermal annealing and FLA

The average sheet resistance of the as deposited films was 50 Ω/sq. After TA or FLA the sheet resistance decreases as shown in figure 11 with the lowest resistance achieved being 29 Ω/sq. This sheet resistance was achieved by TA alone at 215 °C for 30 minutes and at 155 °C for 5 minutes with FLA treatment. The sheet resistance or resistivity of the film depends on both the carrier concentration and the mobility. For FLA the sheet resistance drops initially due to the increase in carrier concentration but later is attributed to the increase in carrier mobility. For TA as the annealing time increases the sheet resistance drops, which is mainly due to the stark increase in mobility. For either treatment, as the time or pulse count increases the sheet resistance decreases. Using the combination of TA and FLA only has substantial effect for annealing at 155 °C and 190 °C for 5 minutes, otherwise the sheet resistance saw minimal change after the TA. FLA does not offer much improvement in the electrical properties after TA since thermal annealing transfers a large amount of energy to the lattice which is sufficient to promote crystallization and removal of many defects. FLA is a high energy process that only last a short time so after thermal annealing FLA does not provide enough energy to further promote crystal growth or removal of significant defects.

The optical bandgap seen in figure 12 shifts to shorter wavelengths (higher energies) after both FLA and TA. The higher the pulse count the larger the shift in the optical bandgap as expected since a larger pulse count corresponds to more energy being deposited in the film and more crystallization occurring as shown by XRD analysis. Thermal annealing similarly shifts the bandgap to lower wavelengths. At 190 °C annealing for more than 15 minutes has no effect on the optical bandgap. The benefit of increasing temperature appears to reach a plateau at around 190 °C since annealing at 215 °C causes no further shift in the bandgap. 3.8 eV is the max bandgap achieved through either TA or FLA. Combining flash lamp annealing and thermal annealing does not cause an increase in the bandgap beyond what either treatment can achieve individually as seen in figure 12.

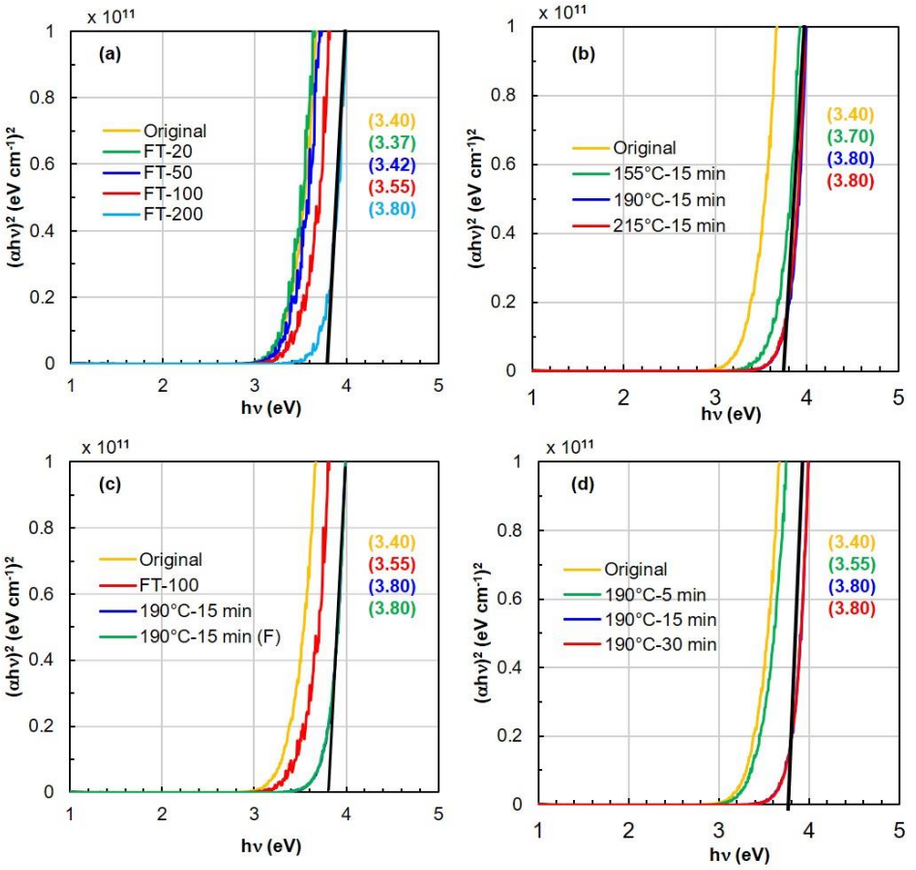

Figure 12: Optical bandgap for a) different flash annealing conditions b) different thermal annealing temperatures c) comparison of annealing methods d) different thermal annealing times

Absorption coefficient was calculated using Beer-Lamberts law (equation 2). R in equation 2 is the reflectance, T is the Transmittance and t is the film thickness.

$$\alpha = \frac{1}{t}\ln\left(\frac{100-R}{T}\right) \qquad (2)$$

Optical bandgap was subsequently graphed using equation 3 [7, 24]. In equation 3 α is the absorption coefficient, $h\nu$ is the photon energy and E_g is the optical bandgap.

$$(\alpha h\nu)^2 = h\nu - E_g \qquad (3)$$

ITO is a degenerate semiconductor, so the widening of the bandgap is often attributed to the Moss-Burstein effect which is due to increased carrier concentration [3]. Here it was found that the bandgap widens after TA or FLA but the carrier concentration typically decreases. For FLA with a pulse count of 20 or 50 the carrier concentration increases but the bandgap does not change substantially from the as-deposited sample so the Moss-Burstein effect does not play a dominating role. The defect in the as-deposited film causes intermediate donor levels which effectively lower the bandgap so when these defects are removed the donor levels are removed and the bandgap effectively widens. Joshi, Salil M., et al in [2] state that doping with Sn causes oxygen vacancies which create shallow donor states close to the conduction band. It is hypothesized that during TA or FLA at high pulse counts oxygen vacancies are removed, which would remove these shallow donor states and account for the widening of the optical bandgap. This is supported by other research which similar suggests that removal of oxygen vacancies which act as shallow donors allows for widening of the bandgap [21].

Transmittance remains constant under FLA until a pulse count of 200 as shown in figure 13. For a pulse count of 200 there is an increase in transmission over most of the spectrum but most significantly in the ultraviolet (UV) and infrared regions (IR). TA increases the transmittance as shown in figure 13(b, c) where a higher/longer annealing temperatures/times corresponds to higher transmittance. Again, the transmittance increases somewhat over the entire spectrum most significantly in the UV and IR regions. The transmittance in the visible region increases slightly with high annealing temperature or pulse count but otherwise remains unchanged. Looking at figure 13(e) FLA after TA does not change the transmission.

In [6] it is suggested that a lower carrier concentration leads to higher transmittance in the IR region due to less carriers being available to scatter the light. In [25] they found decreasing transmittance in the IR region with increasing carrier concentration which is in agreement with our findings. A decrease in carrier concentration was found which would account for the increase in transmittance in the IR region. The

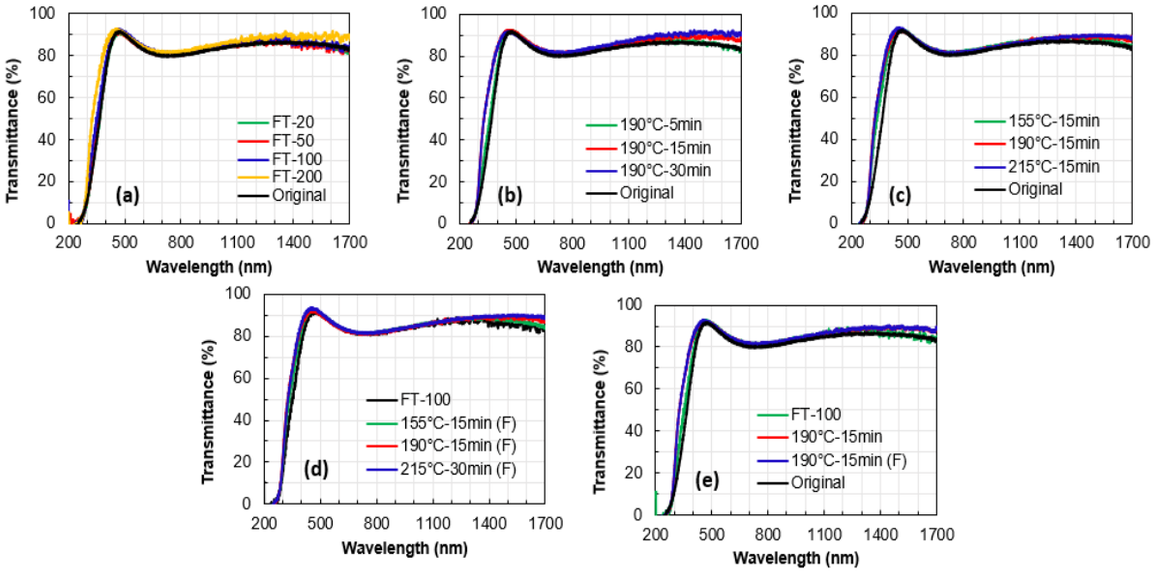

Figure 13. Transmission spectrum for a) different flash annealing conditions b) different thermal annealing temperatures c) different thermal annealing lengths d) thermal annealing and flash annealing e) comparison of all three annealing methods

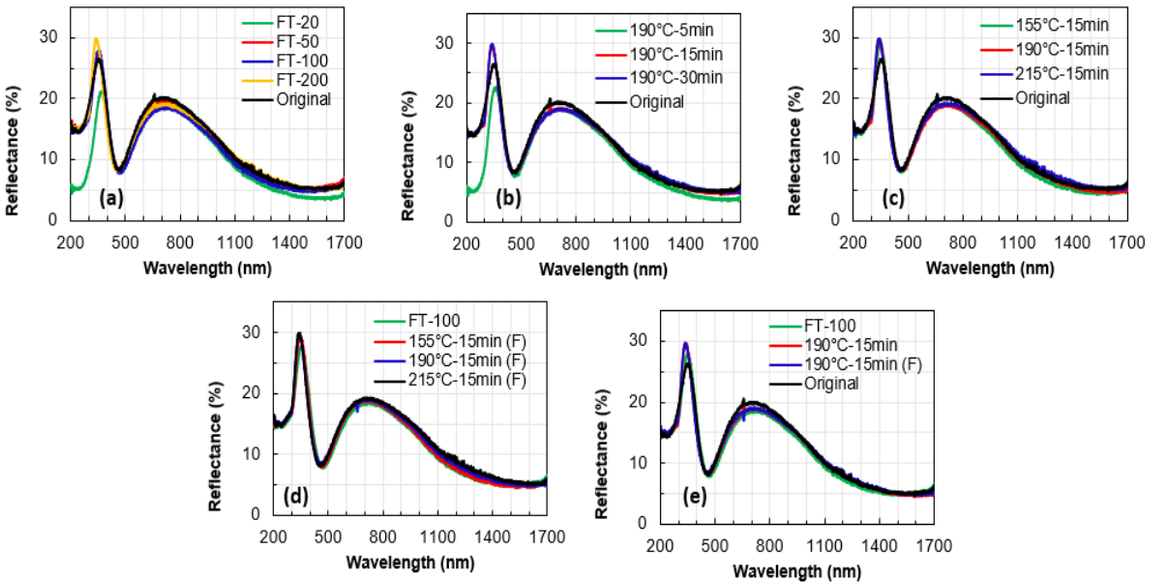

Figure 14: Reflectance spectrum for a) different flash annealing conditions b) different thermal annealing temperatures c) different thermal annealing lengths d) thermal annealing and flash annealing e) comparison of all three annealing treatments

transmittance increase in the UV region is explained by the widening of the bandgap, allowing higher energy photons to be transmitted. The slight increase in the transmittance over the visible spectrum is believed to be due to the decrease in oxygen vacancies as indicated by the decrease in carrier concentration.

Figure 14 shows the reflection spectrum for various annealing conditions. The reflectance decreases over the visible and IR regions for both FLA and TA. This reduction in reflection is accompanied by a increase in the transmittance. At an annealing time of 15 minutes the reflectance is unchanged for different annealing temperatures. For all annealing conditions there is an increase in the reflectance in the range of 300-400 nm. This increase in reflection could be due to reduced absorption accompanied by the widening of the bandgap. The reflectance increase with annealing temperature as in figure 14(c). The annealing time appears to reach saturation at or before 15 minutes since there is no further change in the reflectance for increased annealing time.

For the FLA treatment with pulse count of 20 and the TA treatment at 190°C for 5 minutes, there is about a 10% decrease in the reflection in the UV region and a smaller decrease in the IR. This reduction in reflection is accompanied by a corresponfing increase in the transmittance spectrum for the sample TA at 190°C for 5 minutes. The transmittance spectrum for the FLA of 20 however does not see any increase. For both these conditions there is a increase in the carrier concetration as indicated in figure 9(a, c). The mechanism for this decrease in relfectance in the UV region for FLA with a pulse count of 20 is unexpected and requires futher characterization.

FLA after TA has minimal effect on the reflection spectrum for ITO. The lack of change in the transmission or reflection with the combined annealing treatment is attributed to the lack of significant change to the crytal structure of the film with the additional FLA treatment.

IV. CONCLUSION

Comparison of the electrical properties, optical properties, and morphology of ITO films post processed by FLA and TA were conducted. 100 nm thick ITO films underwent flash lamp annealing and thermal annealing. XRD analysis showed that FLA can crystallize ITO under high pulse count. The crystal size of the ITO films did not vary substantially between FLA or TA samples. The sheet resistance was decreased substantially with both FLA and TA, achieving a resistance of 29 Ω/sq. The mobility increased from 30-40 to 70-80 $cm^2\,V^{-1}s^{-1}$ for FLA and TA as the film shifted from amorphous to crystalline and defects were removed. The carrier concentration decreased for TA and for FLA due to oxygen vacancies being removed. By tuning the parameters of FLA ITO films with similar electrical and optical properties to TA samples is achievable. The sequential treatment by TA at low temperatures followed by FLA can be used to achieve better film properties than thermal annealing alone at longer and higher temperatures. The combination or sequential

treatment via TA and FLA offers improved film properties and lower processing time. Given FLA performance on creating quality ITO films on glass and its low temperature nature it offers an appealing solution for processing of ITO films on temperature sensitive substrates. FLA offers a much faster processing time than TA which makes it especially interesting for production applications.

ACKNOWLEDGMENTS

We acknowledge the support of National Science Foundation award number 2243110. Ethan Neitzke would like to thank Mr. David Stevenson of Ampres Inc for teaching him how to use the Novacentrix PF-3300 flash lamp system. The authors would also like to thank Thanh Tran (CHEMS Department, MSU) and Dr. Per Askeland (Composite Materials and Structures Center, MSU) for SEM measurements and Xiaobo Wang (CHEMS Department, MSU) for XRD measurements.

STATEMENT OF DATA AVAILABILITY

The data supporting the findings presented here are available upon reasonable request from corresponding author.

CONFLICT OF INTEREST STATEMENT

The Authors have no conflicts to disclose.

REFERENCES

[1] Schube, Jörg, et al. "Intense Pulsed Light in Back End Processing of Solar Cells with Passivating Contacts Based on Amorphous or Polycrystalline Silicon Layers." *Solar Energy Materials and Solar Cells*, vol. 216, 2020, p. 110711, https://doi.org/10.1016/j.solmat.2020.110711.

[2] Joshi, Salil M., et al. "A Comparative Study of the Effect of Annealing and Plasma Treatments on the Microstructure and Properties of Colloidal Indium Tin Oxide Films and Cold-Sputtered Indium Tin Oxide Films." *Thin Solid Films*, vol. 520, no. 7, 2012, pp. 2723–2730, https://doi.org/10.1016/j.tsf.2011.11.052.

[3] Han, H., et al. "Band Gap Shift in the Indium-Tin-Oxide Films on Polyethylene Napthalate after Thermal Annealing in Air." *Journal of Applied Physics*, vol. 100, no. 8, 2006, https://doi.org/10.1063/1.2357647.

[4] Ahmed, Naser M., et al. "The Effect of Post Annealing Temperature on Grain Size of Indium-Tin-Oxide for Optical and Electrical Properties Improvement." *Results in Physics*, vol. 13, 2019, p. 102159, https://doi.org/10.1016/j.rinp.2019.102159.

[5] Farid, N, et al. "Improvement of electrical properties of ito thin films by melt-free ultra-short laser crystallization." *Journal of Physics D: Applied Physics*, vol. 54, no. 18, 2021, p. 185103, https://doi.org/10.1088/1361-6463/abe2c6.

[6] Hu, Yalan, et al. "Effects of heat treatment on properties of ITO Films prepared by RF Magnetron Sputtering." *Vacuum*, vol. 75, no. 2, 2004, pp. 183–188, https://doi.org/10.1016/j.vacuum.2004.01.081.

[7] Eshaghi, Akbar, and Alireza Graeli. "Optical and Electrical Properties of Indium Tin Oxide (Ito) Nanostructured Thin Films Deposited on Polycarbonate Substrates 'Thickness Effect.'" *Optik*, vol. 125, no. 3, 2014, pp. 1478–1481, https://doi.org/10.1016/j.ijleo.2013.09.011.

[8] Guillot, Martin J., et al. "Simulating the thermal response of thin films during photonic curing." *Volume 7: Fluids and Heat Transfer, Parts A, B, C, and D*, 2012, https://doi.org/10.1115/imece2012-87674.

[9] Druffel, Thad, et al. "Intense pulsed light processing for photovoltaic manufacturing." *Solar Energy Materials and Solar Cells*, vol. 174, 2018, pp. 359–369, https://doi.org/10.1016/j.solmat.2017.09.010.

[10] Ryu, Jongeun, et al. "Reactive Sintering of Copper Nanoparticles Using Intense Pulsed Light for Printed Electronics." *Journal of Electronic Materials*, vol. 40, no. 1, 2010, pp. 42–50, https://doi.org/10.1007/s11664-010-1384-0.

[11] Abbel, Robert, et al. "Industrial-Scale Inkjet Printed Electronics Manufacturing—Production up-Scaling from Concept Tools to a Roll-to-Roll Pilot Line." *Translational Materials Research*, vol. 1, no. 1, 2014, p. 015002, https://doi.org/10.1088/2053-1613/1/015002.

[12] Schube, Jorg, et al. "Intense Pulsed Light Meets the Metallization of Silicon Heterojunction Solar Cells." *2019 IEEE 46th Photovoltaic Specialists Conference (PVSC)*, 2019, https://doi.org/10.1109/pvsc40753.2019.8981314.

[13] Kim, Yoonsuk, Seungho Park, Seok Kim, Byung Kuk Kim, Yujin Choi, et al. "Flash lamp annealing of indium tin oxide thin-films deposited on polyimide backplanes." *Thin Solid Films*, vol. 628, 2017, pp. 88–95, https://doi.org/10.1016/j.tsf.2017.03.016.

[14] Kim, Yoonsuk, Seungho Park, Byung-Kuk Kim, Hyoung June Kim, and Jin-Ha Hwang. "Xe-arc flash annealing of indium tin oxide thin-films prepared on glass backplanes." *International Journal of Heat and Mass Transfer*, vol. 91, 2015, pp. 543–551, https://doi.org/10.1016/j.ijheatmasstransfer.2015.07.132.

[15] Wünscher, Sebastian, et al. "Progress of Alternative Sintering Approaches of Inkjet-Printed Metal Inks and Their Application for Manufacturing of Flexible Electronic Devices." *J. Mater. Chem. C*, vol. 2, no. 48, 2014, pp. 10232–10261, https://doi.org/10.1039/c4tc01820f.

[16] Guillot, Martin J., et al. "Simulating the Thermal Response of Thin Films during Photonic Curing." *Volume 7: Fluids and Heat Transfer, Parts A, B, C, and D*, 2012, https://doi.org/10.1115/imece2012-87674.

[17] Ghorannevis, Z., et al. "Structural and Morphological Properties of Ito Thin Films Grown by Magnetron Sputtering." *Journal of Theoretical and Applied Physics*, vol. 9, no. 4, 2015, pp. 285–290, https://doi.org/10.1007/s40094-015-0187-3.

[18] Ding, Zhanlai, et al. "Preparation of Ito Nanoparticles by Liquid Phase Coprecipitation Method." *Journal of Nanomaterials*, vol. 2010, 2010, pp. 1–5, https://doi.org/10.1155/2010/543601.

[19] Ahmed, Naser M., et al. "The effect of post annealing temperature on grain size of indium-tin-oxide for optical and Electrical Properties Improvement." *Results in Physics*, vol. 13, 2019, p. 102159, https://doi.org/10.1016/j.rinp.2019.102159.

[20] Kikuchi, Naoto, et al. "Phonon scattering in electron transport phenomena of Ito Films." *Vacuum*, vol. 59, no. 2–3, 2000, pp. 492–499, https://doi.org/10.1016/s0042-207x(00)00307-9.

[21] Buckeridge, J., et al. "Deep vs Shallow Nature of Oxygen Vacancies and Consequent n-Type Carrier Concentrations in Transparent Conducting Oxides." *Physical Review Materials*, vol. 2, no. 5, 2018, https://doi.org/10.1103/physrevmaterials.2.054604.

[22] Han, H., et al. "Band Gap Shift in the Indium-Tin-Oxide Films on Polyethylene Napthalate after Thermal Annealing in Air." *Journal of Applied Physics*, vol. 100, no. 8, 2006, https://doi.org/10.1063/1.2357647.

[23] Kim, Jiwoong, et al. "High-Temperature Optical Properties of Indium Tin Oxide Thin-Films." *Scientific Reports*, vol. 10, no. 1, 2020, https://doi.org/10.1038/s41598-020-69463-4.

[24] Huh, Myung Soo, et al. "Improving the Morphological and Optical Properties of Sputtered Indium Tin Oxide Thin Films by Adopting Ultralow-Pressure Sputtering." *Journal of The Electrochemical Society*, vol. 156, no. 1, 2009, https://doi.org/10.1149/1.3005562.

[25] Lee, Ho-Chul, and O Ok Park. "Electron scattering mechanisms in indium-tin-oxide thin films: Grain boundary and ionized impurity scattering." *Vacuum*, vol. 75, no. 3, 2004, pp. 275–282, https://doi.org/10.1016/j.vacuum.2004.03.008.

Journal of Applied Physics

AIP Publishing

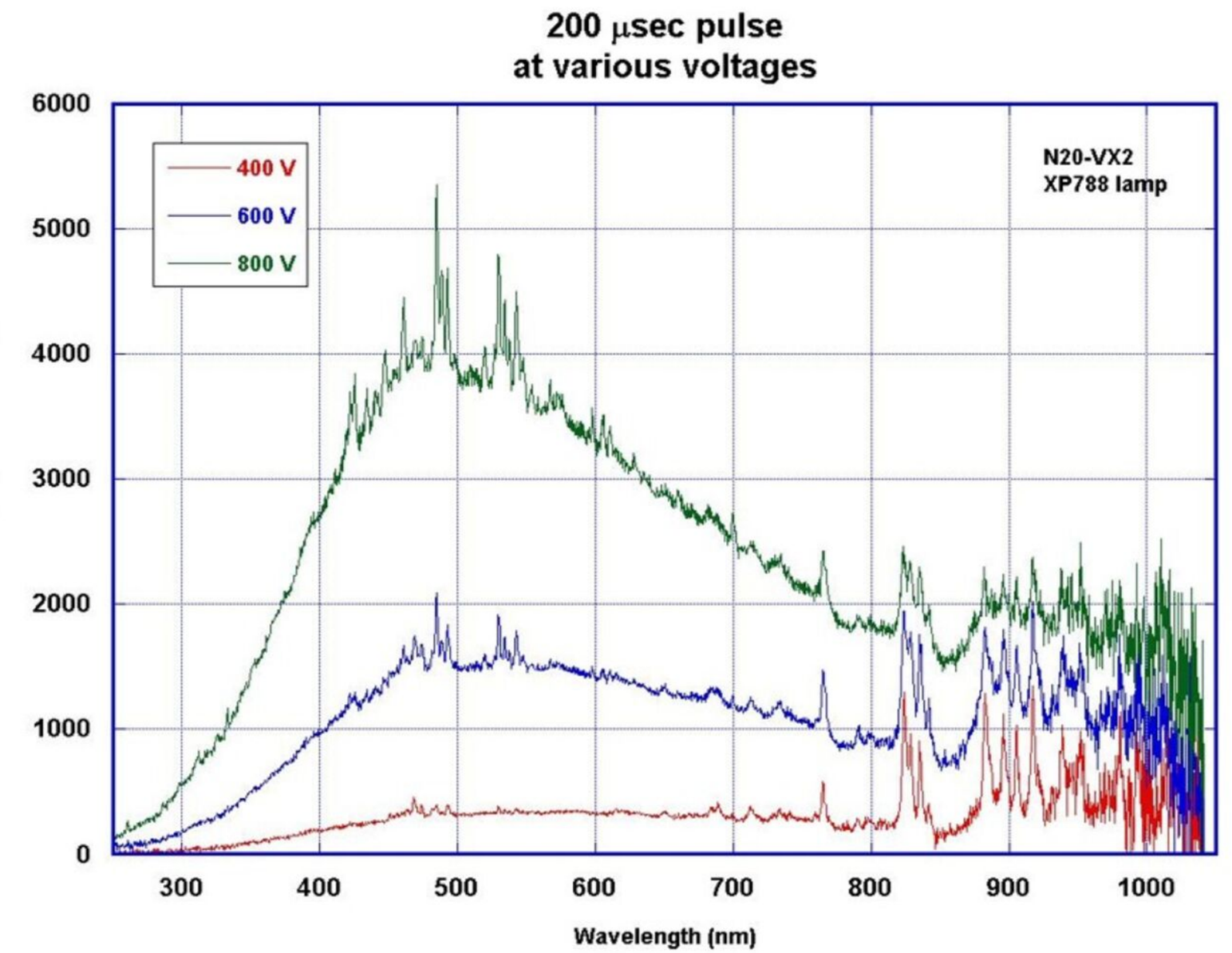

AIP Publishing

Journal of Applied Physics

ACCEPTED MANUSCRIPT

PLEASE CITE THIS ARTICLE AS DOI: 10.1063/5.0177627

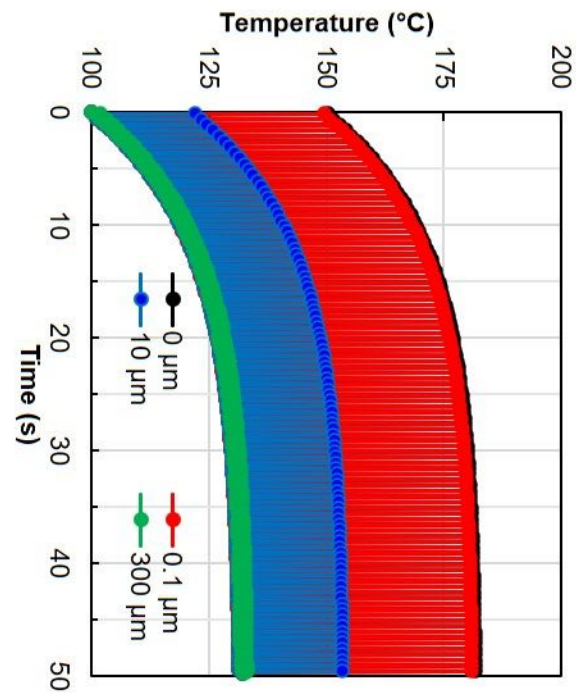

AIP Publishing

Journal of Applied Physics

ACCEPTED MANUSCRIPT

PLEASE CITE THIS ARTICLE AS DOI: 10.1063/5.0177627

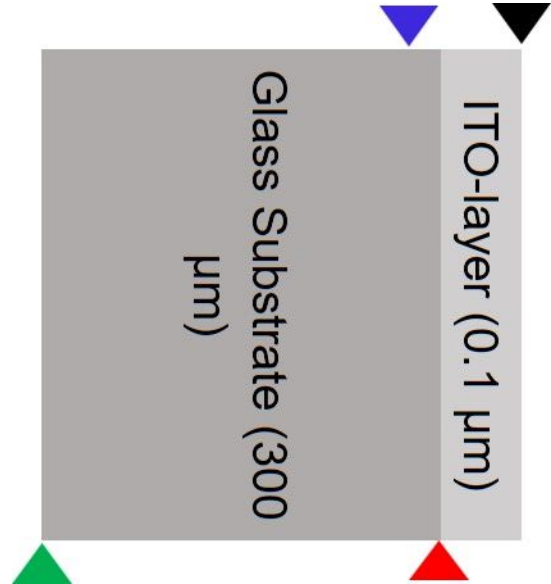

AIP Publishing

Journal of Applied Physics

ACCEPTED MANUSCRIPT

PLEASE CITE THIS ARTICLE AS DOI: 10.1063/5.0177627

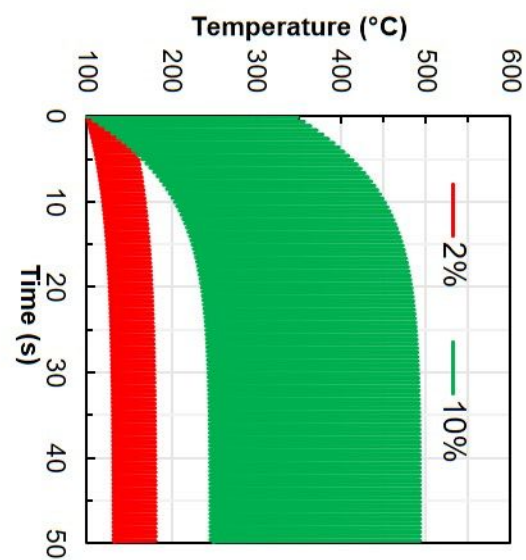

AIP Publishing

Journal of Applied Physics

ACCEPTED MANUSCRIPT

PLEASE CITE THIS ARTICLE AS DOI: 10.1063/5.0177627

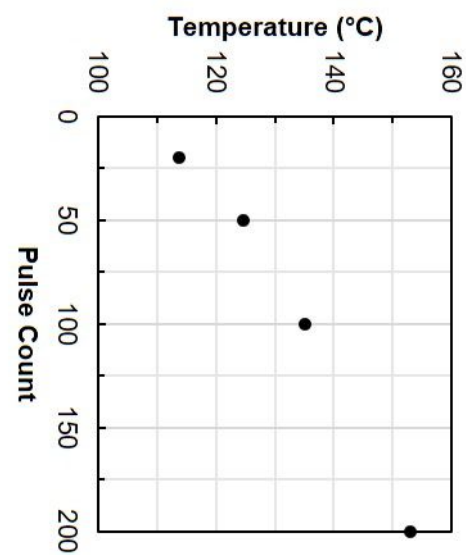

AIP Publishing

Journal of Applied Physics

ACCEPTED MANUSCRIPT

This is the author's peer reviewed, accepted manuscript. However, the online version of record will be different from this version once it has been copyedited and typeset.
PLEASE CITE THIS ARTICLE AS DOI: 10.1063/5.0177627

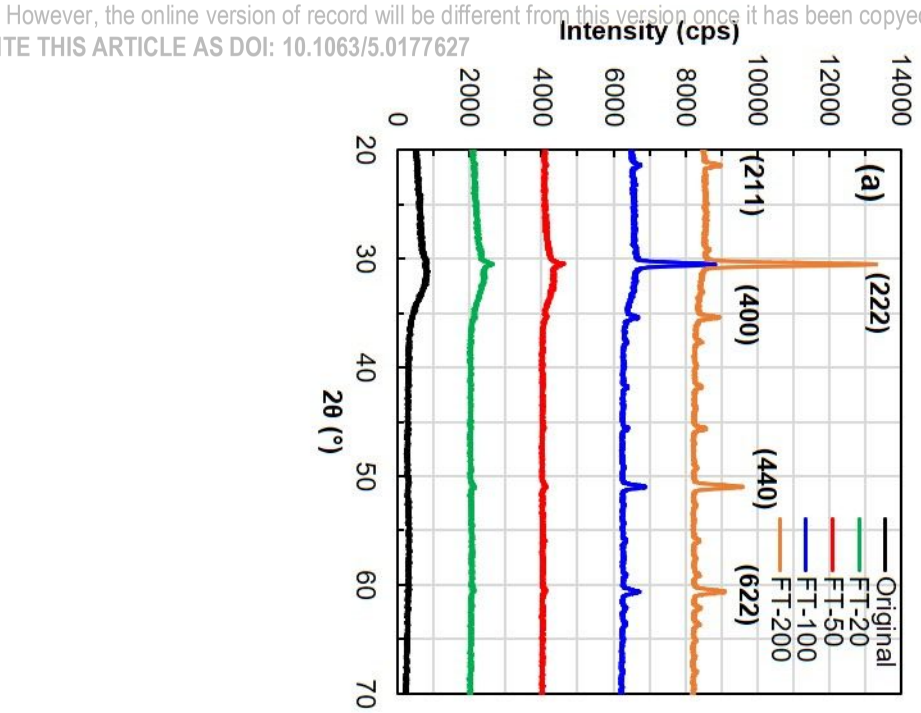

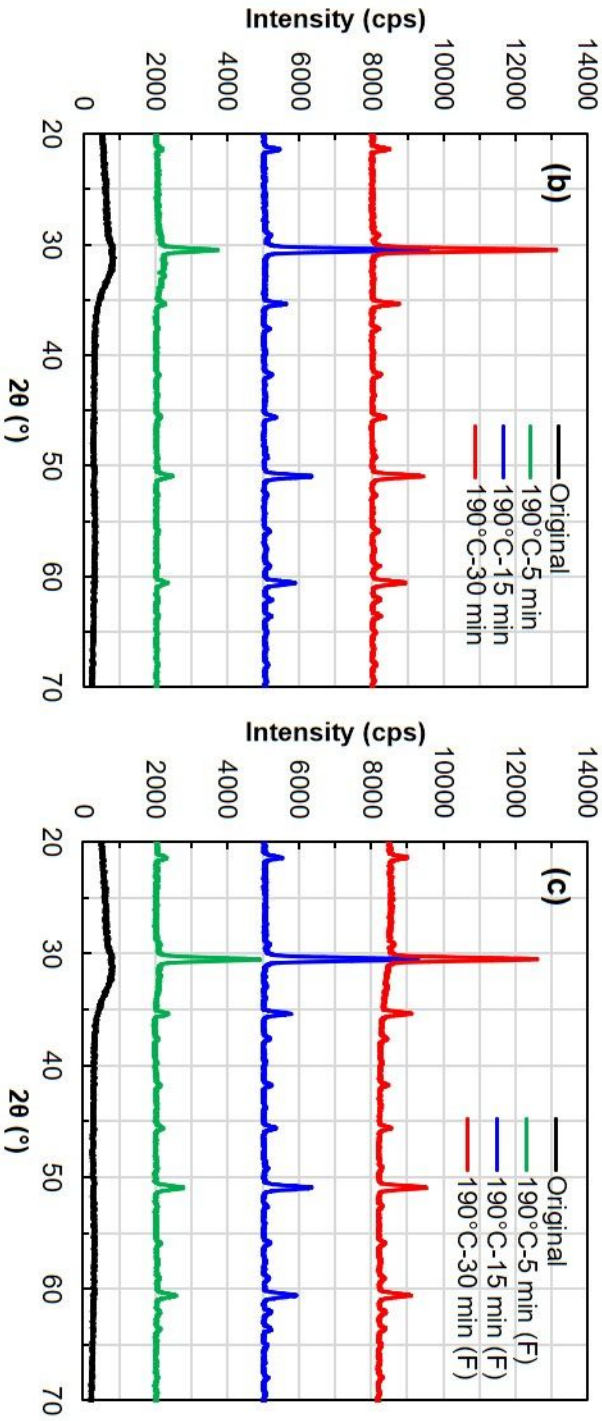

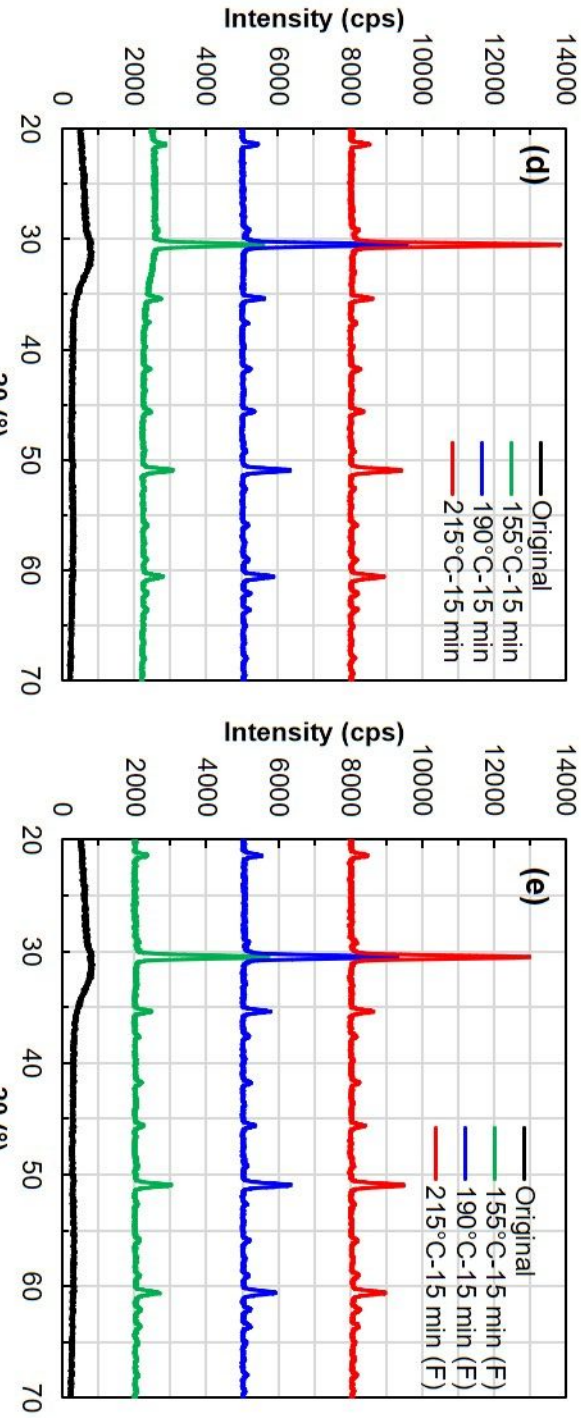

AIP Publishing

Journal of Applied Physics

ACCEPTED MANUSCRIPT

This is the author's peer reviewed, accepted manuscript. However, the online version of record will be different from this version once it has been copyedited and typeset.
PLEASE CITE THIS ARTICLE AS DOI: 10.1063/5.0177627

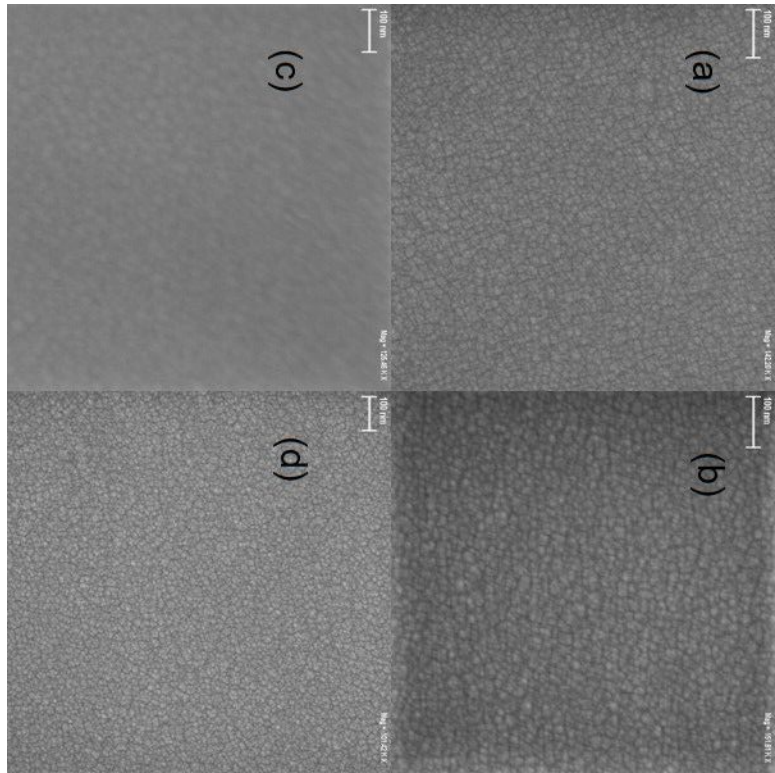

Journal of Applied Physics

AIP Publishing

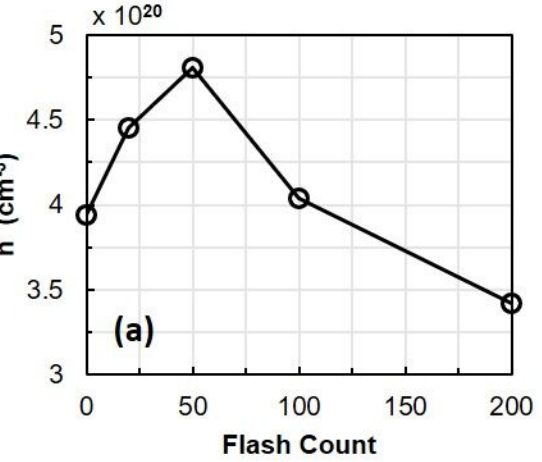

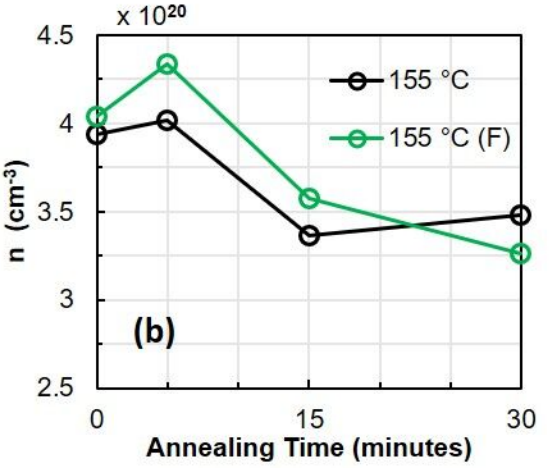

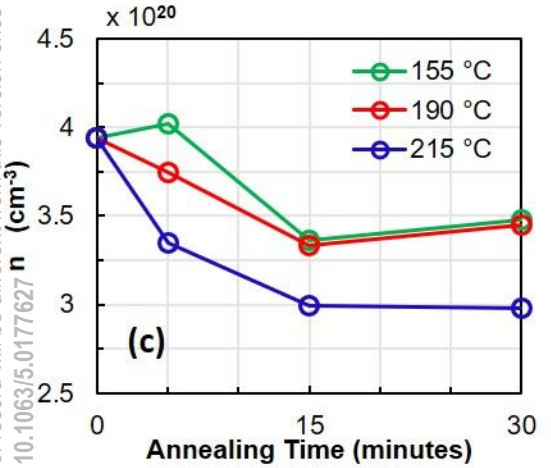

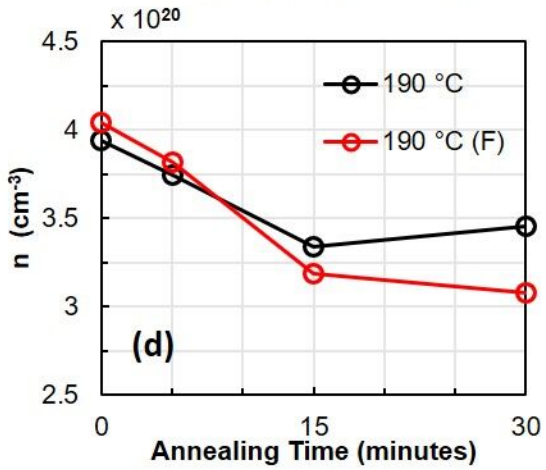

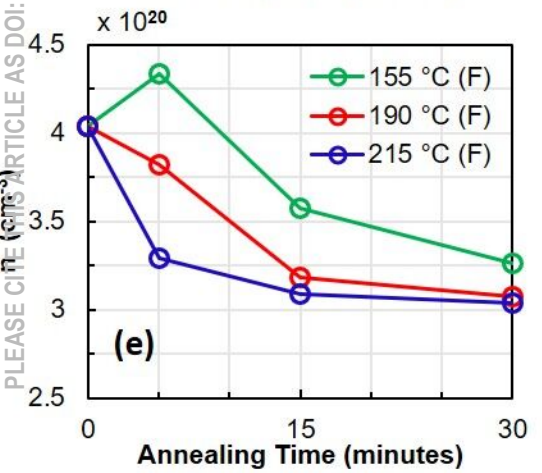

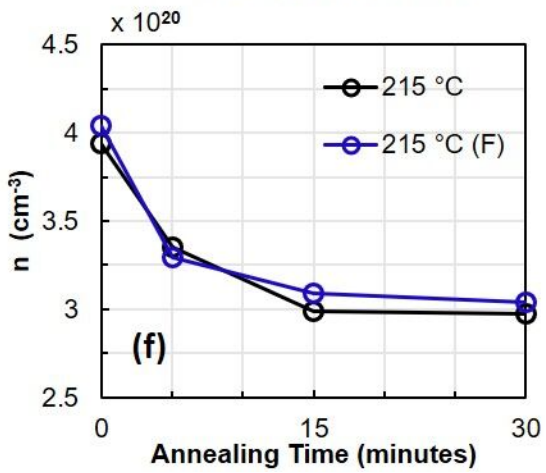

Journal of Applied Physics

AIP Publishing

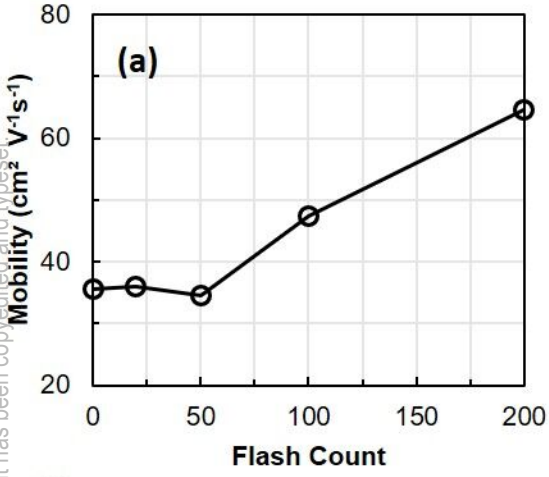

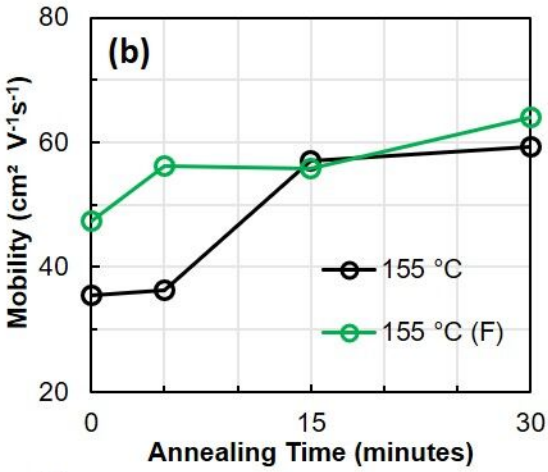

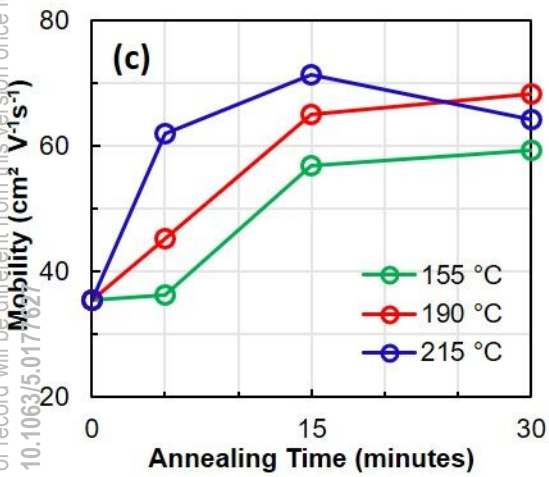

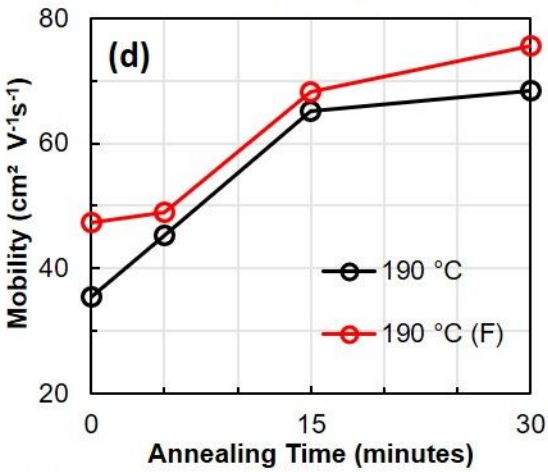

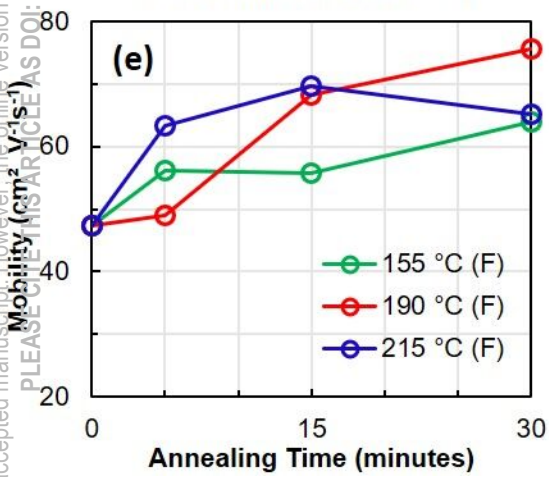

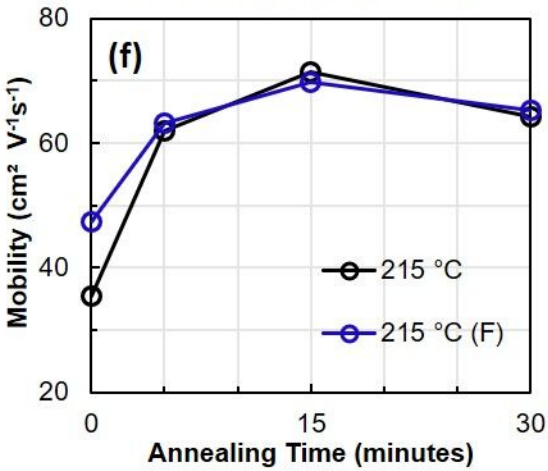

Journal of Applied Physics

AIP Publishing

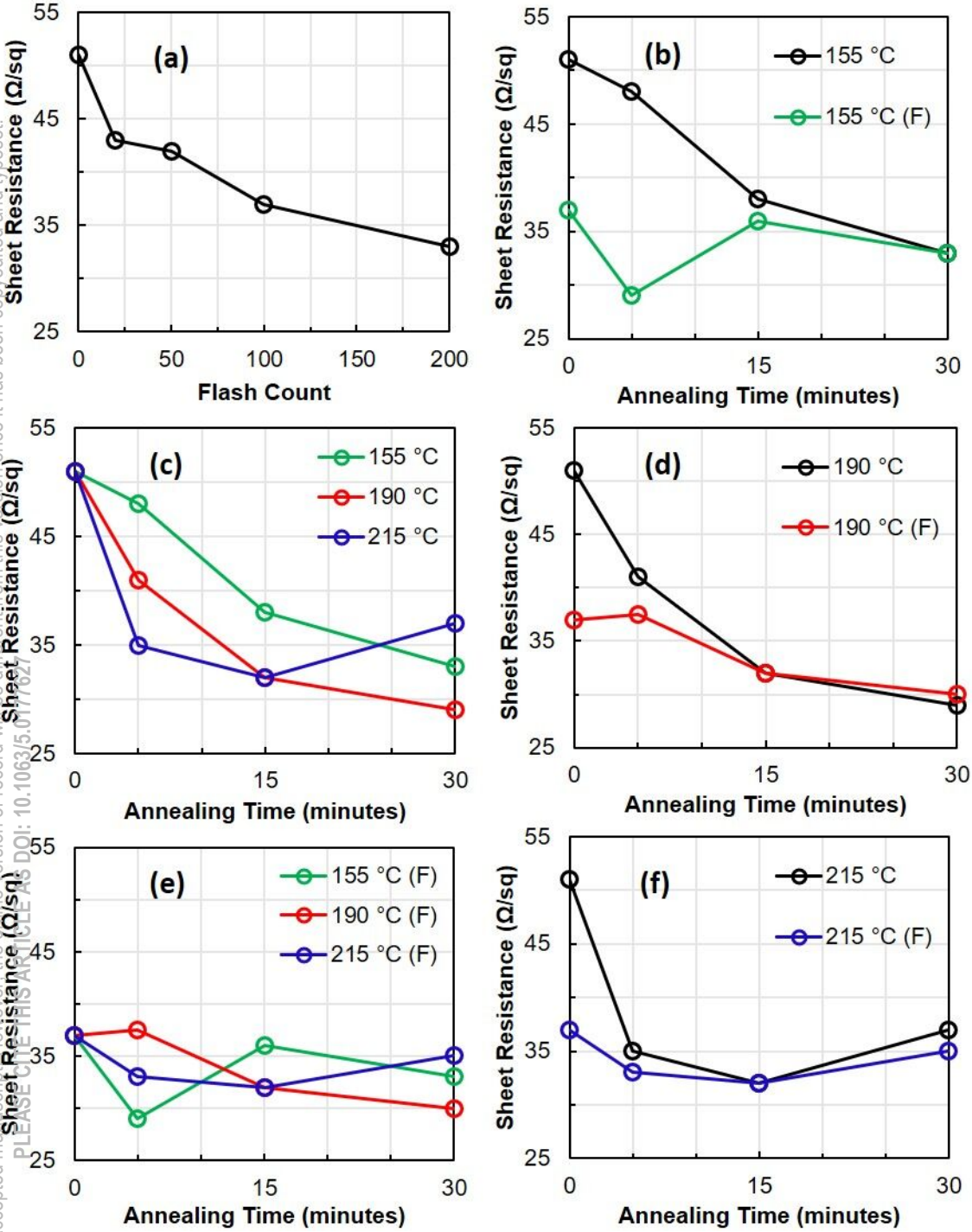

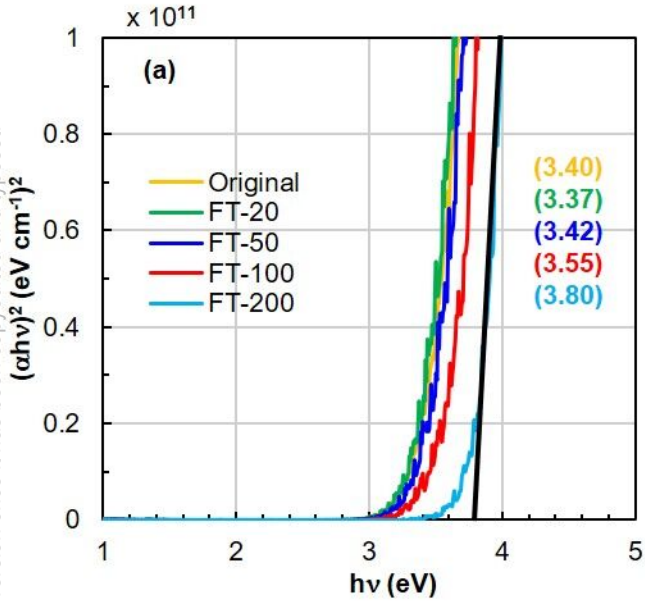

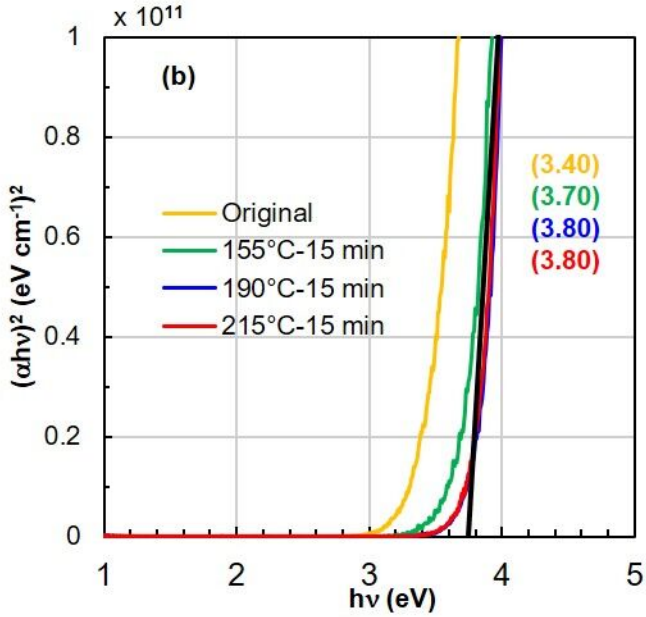

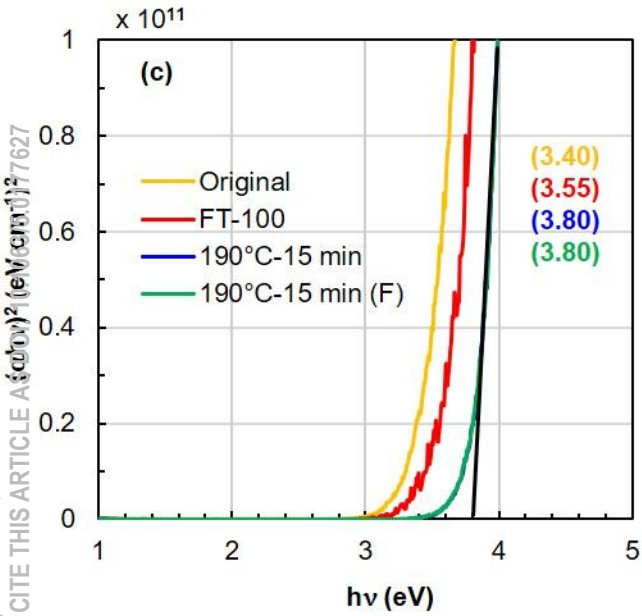

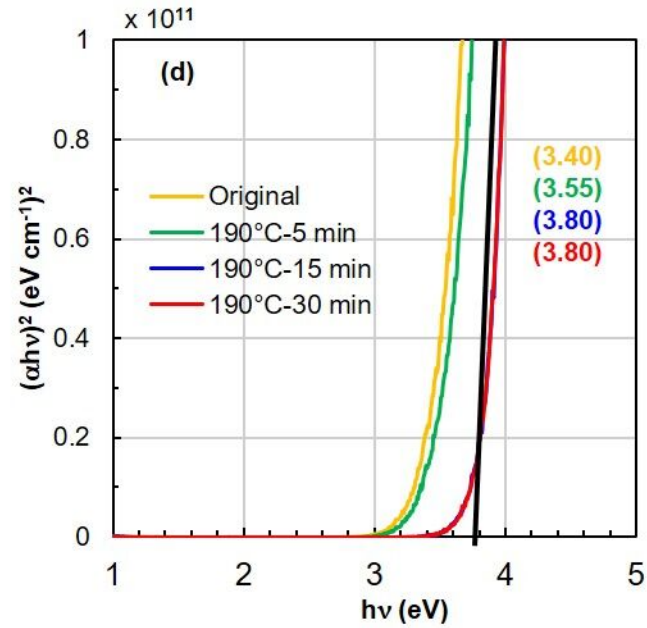

AIP Publishing

Journal of Applied Physics

ACCEPTED MANUSCRIPT

This is the author's peer reviewed, accepted manuscript. However, the online version of record will be different from this version once it has been copyedited and typeset.
PLEASE CITE THIS ARTICLE AS DOI: 10.1063/5.0177627

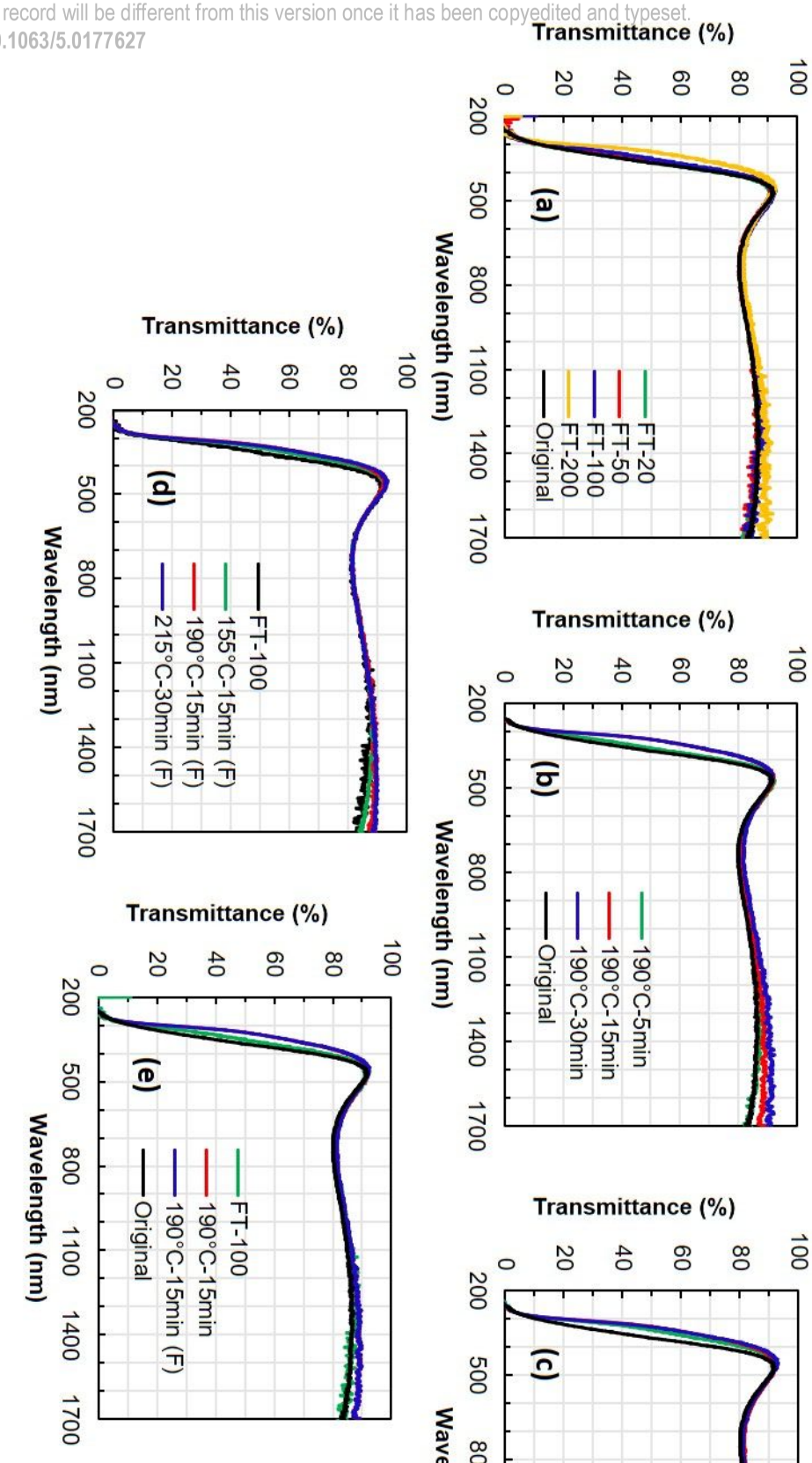

Journal of Applied Physics

AIP Publishing